



# Mapping the Mechanical Properties of Alloyed Magnesium (AZ 61)

## Application Note

Jennifer Hay, Phil Agee, and Dr. Hamdallah Bearat  
Agilent Technologies

### Introduction

Behind iron and aluminum, magnesium (Mg) is the third most common element used in engineered structures, because it is light-weight, stiff, and strong [1]. Alloying with aluminum can further improve stiffness and strength, although bulk mechanical properties depend strongly on chemical composition and thermo-mechanical history, insofar as these parameters affect microstructure. In this work, we use nanoindentation to determine the properties of individual phases within a popular magnesium alloy, AZ 61.

AZ 61 is a commercially available magnesium alloy which includes aluminum (nominally 6%), zinc (nominally 1%), and other trace elements. Table 1 provides the chemical composition for AZ 61[2]. The zinc and other trace elements have little effect on microstructure,

| Element   | % by mass |
|-----------|-----------|
| Aluminum  | 5–7       |
| Zinc      | 0.8–1     |
| Copper    | < 0.03    |
| Silicon   | < 0.01    |
| Iron      | < 0.01    |
| Nickel    | <0.005    |
| Magnesium | Balance   |

Table 1. Chemical composition of Magnesium AZ 61 alloy[2].

and the Mg-Al phase diagram is employed to predict the constitution of slowly-cooled AZ 61. At 6% Al, the Mg-Al phase diagram predicts the interaction of two phases: an  $\alpha$  phase which is Mg-rich and a  $\beta$  phase comprising the intermetallic compound  $Al_{12}Mg_{17}$ . As the alloy cools from the liquid state, the  $\beta$  phase begins to solidify at about 620°C. Solidification is complete at about 540°C, and at this temperature, the material exists entirely in the  $\alpha$  phase. Beginning around 300°C, the  $\beta$  phase begins to precipitate and the mass fraction of this secondary phase continues to grow as the material continues to cool. At temperatures below 100°C, the  $\beta$  phase accounts for about 7.5% of the material[3].

In this work, we used nanoindentation to measure the elastic modulus and hardness of both phases of AZ 61. Our expectation is that the modulus for each phase should be close to that for the primary component. The primary component of the  $\alpha$  phase is Mg, which has an elastic modulus of 45 GPa[1]; however, it should be remembered that at room temperature, the  $\alpha$  phase does include 3% of interstitial aluminum (by mass). Thus, we should not be surprised if the modulus of the  $\alpha$  phase is slightly higher than 45 GPa. Zhang et al.



calculated the elastic modulus of the  $\text{Al}_{12}\text{Mg}_{17}$  to be 78 GPa from first principles[4], so this value sets our expectations for the  $\beta$  phase of AZ 61.

In this work, we used Agilent's Express Test option which implements traditional indentation testing in a revolutionary way in order to achieve unprecedented testing speeds. Express Test performs one complete indentation cycle per second, including approach, contact detection, load, unload, and movement to the next indentation site[5]. One important feature of Express Test is the ability to quantitatively "map" both the elastic modulus and the hardness of a surface in a reasonable time. This feature is particularly beneficial for probing multi-phase metals such as AZ 61.

### Experimental Method

The sample of AZ 61 tested in this work was prepared by researchers at the Material Science and Engineering Department at Drexel University. AZ 61 chunks were purchased from Thixomat (Livonia, MI). The chunks were placed in alumina crucibles which were covered with alumina disks. Then the crucibles were placed in a vacuum furnace and were heated with a rate of  $10^\circ\text{C}/\text{min}$  up to  $750^\circ\text{C}$  and held for one hour at the temperature after which the furnace was turned off and the samples were furnace cooled. To polish the surface, a section was cut from the sample, mounted, and rough ground with water using silicon carbide, beginning with 400-grit and finishing with 1200-grit (US). The samples were polished using  $6\ \mu\text{m}$  and  $1\ \mu\text{m}$  diamond on a medium nap cloth with an alcohol-based extender.

Scanning electron microscopy was performed with the Agilent 8500 Field Emission Scanning Electron Microscope (FE-SEM). The prepared sample was fixed to an SEM stub

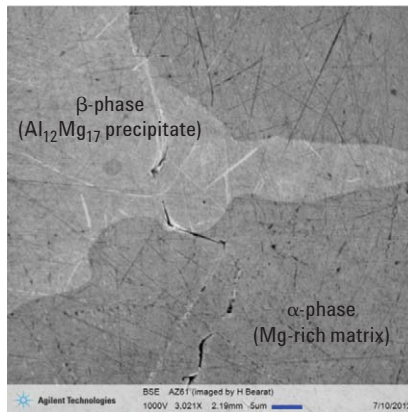


Figure 1. Low-voltage, field-emission, scanning-electron-microscopy (LV FE-SEM) image of Mg AZ 61 as prepared for nanoindentation. Acquired in back-scattered electron (BSE) mode. Image resolution is  $1024 \times 1024$  pixels. Smaller scratches in the  $\beta$  phase evidence higher hardness.

with carbon tape and mounted onto the SEM sample stage. Imaging was performed with the slowest scan speed, in backscattered electron mode, with an accelerating voltage of 1kV. The working distance was 2.2mm.

All indentation testing was performed with an Agilent G200 NanoIndenter having Express Test, NanoVision, and a DCM II fitted with a Berkovich

indenter. The test method "Express Test to a Force" was used to perform an array of  $20 \times 20$  indents within a  $50\ \mu\text{m} \times 50\ \mu\text{m}$  area; thus, the separation between successive indents was about  $2.5\ \mu\text{m}$  ( $2500\ \text{nm}$ ). The peak force for every indent was 4 mN; in the  $\alpha$  phase, this force produced a peak displacement of about  $380\ \text{nm}$ ; in the  $\beta$  phase, this force produced a peak displacement of about  $240\ \text{nm}$ .

### Results and Discussion

The scanning-electron microscopic (SEM) image of Figure 1 shows the microstructure of the AZ 61 surface as prepared for indentation. The  $\alpha$  phase is darker and the precipitated  $\beta$  phase is lighter. From this image alone, one deduces that the  $\beta$  phase is harder, because scratches that span both phases are smaller in the  $\beta$  phase.

Figure 2 shows the maps of elastic modulus and hardness generated by a  $20 \times 20$  array of indentations. The total testing time is 15 minutes. Each indentation generates the information content for one pixel; thus, the images in Figure 2 are 400-pixel

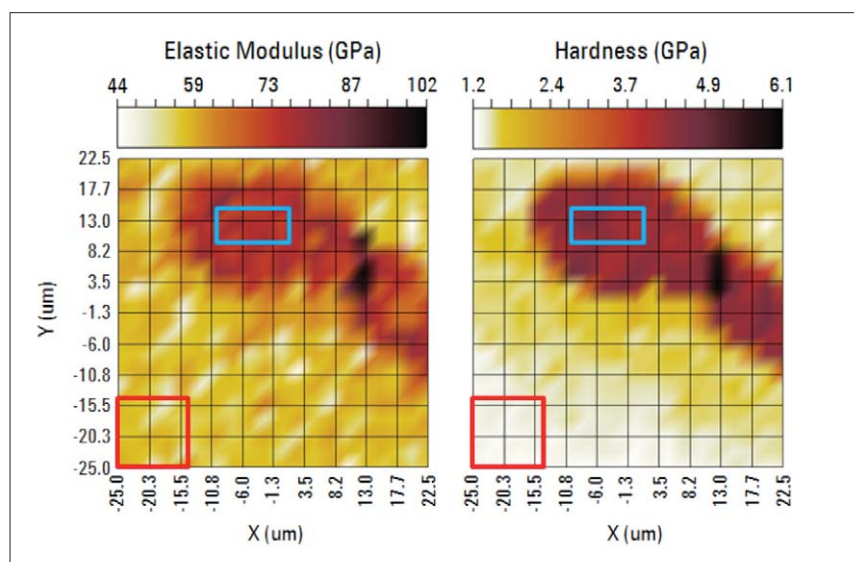


Figure 2. Modulus and hardness of two-phase Mg AZ 61. Red rectangles are in the primary  $\alpha$  phase (Mg-rich). Blue rectangles are in the  $\beta$  phase ( $\text{Al}_{12}\text{Mg}_{17}$ ). Information for both images was acquired in 15 minutes by means of Express Test. Image resolution is  $20 \times 20$  pixels.

| Material   | Present work<br>4 mN applied force |                         |                         | Relevant<br>Comparisons           |          |     |
|--|------------------------------------|-------------------------|-------------------------|-----------------------------------|----------|-----|
|  | N                                  | E<br>(std. dev.)<br>GPa | H<br>(std. dev.)<br>GPa | Material                          | E<br>GPa | Ref |
| $\alpha$ -phase (Mg-rich)                                | 25                                 | 54.9 (3.3)              | 1.35 (0.05)             | Mg                                | 45       | [1] |
| $\beta$ -phase (Al <sub>12</sub> Mg <sub>17</sub> -rich) | 15                                 | 75.8 (3.3)              | 4.30 (0.19)             | Al <sub>12</sub> Mg <sub>17</sub> | 78       | [4] |

Table 2. Properties of magnesium AZ 61.

(20x20) images. The two phases are clearly distinguished. In order to calculate the properties of each phase independently, two rectangular domains were selected which were clearly in either one phase or the other. These are the red and blue rectangles in Figure 2.

The red rectangle is in the primary  $\alpha$  phase, which is the Mg with interstitial Al that constitutes about 92% of the material. Within the area bound by the red rectangle, there are 25 indentations; the average elastic modulus for these indentations is  $54.9 \pm 3.3$  GPa, which is slightly higher than the modulus of pure Mg (45 GPa). The average hardness is  $1.35 \pm 0.05$  GPa.

The blue rectangle is in the  $\beta$  phase, which is primarily Al<sub>12</sub>Mg<sub>17</sub>. Within the area bound by the blue rectangle, there are 15 indentations; the average elastic modulus for these indentations is  $75.8 \pm 3.3$  GPa, which is consistent with the value predicted by Zhang (78 GPa). The average hardness is  $4.3 \pm 0.19$ , which is about three times greater than the hardness of the  $\alpha$  phase. Table 2 summarizes the properties for each phase.

Surprisingly, the hardness image reveals a region around the  $\beta$  phase in which the hardness is lower than that of the  $\beta$  phase, but higher than that of the  $\alpha$  phase. There are two reasonable explanations for this observation. First, the elevated hardness of the material surrounding the  $\beta$  phase may be caused by (and

reveal)  $\beta$  material immediately below the exposed surface. However, modulus is usually more sensitive to the influence of constraining material, and the modulus is uniform outside the  $\beta$  phase. It must be granted, however, that the difference in hardness between the two phases is much greater than the difference in modulus, so the hardness may manifest more constraint effect than modulus simply because there is a greater difference in hardness between the two phases.

The second (and more interesting) explanation is that the material around the  $\beta$  phase may be a true "mesophase" if it is chemically different than either  $\alpha$  or  $\beta$ . More detailed analysis of the chemistry and microstructure of this region by means of energy dispersive x-ray spectroscopy (EDX), transmission electron spectroscopy (TEM), and focused-ion beam milling (FIB) may shed more light on this phenomenon.

### Conclusions

In this work, the Express Test option for the Agilent G200 NanoIndenter was used to map out the mechanical properties of a magnesium alloy, AZ 61. The measured moduli of the  $\alpha$  and  $\beta$  phases compared well with expected values. The hardness of the precipitate ( $\beta$ ) phase was three times greater than that of the  $\alpha$  phase. The hardness map revealed an area of intermediate hardness surrounding the  $\beta$  phase; more analysis is required to fully explain this phenomenon.

### Acknowledgement

The authors gratefully acknowledge Mr. Babak Anasori and Dr. Michel Barsoum of the Materials Science and Engineering Department of Drexel University for providing the sample of AZ 61 tested in this work.

## References

1. *Magnesium*. [cited 2012 July 9]; Available from: <http://en.wikipedia.org/wiki/Magnesium>.
2. Fang, C.-f., Zhang, X.-g., Ji, S.-h., Jin, J.-z., and Chang, Y.-b., "Microstructure and corrosion property of AZ61 magnesium alloy by electromagnetic stirring," *Trans. Non Ferrous Met. Soc. China* **15**(3), 536-541, 2005.
3. Shackelford, J.F., *Introduction to Materials Science for Engineers*. 2nd ed, p. 223, 1988, New York: Macmillan Publishing Company.
4. Zhang, H., Shang, S.L., Wang, Y., Saengdeejing, A., Chen, L.Q., and Liu, Z.K., "First-principles calculations of the elastic, phonon and thermodynamic properties of Al12Mg17," *Acta Materialia* **58**, 4012–4018, 2010.
5. Hay, J., "Revolutionary New Agilent Express Test Option for G200 NanoIndenters," Agilent Technologies, 2012, Document No: 5990-9948EN, Date Accessed: April 9, 2012; Available from: <http://cp.literature.agilent.com/litweb/pdf/5990-9948EN.pdf>.

## Nanomeasurement Systems from Agilent Technologies

Agilent Technologies, the premier measurement company, offers high-precision, modular nanomeasurement solutions for research, industry, and education. Exceptional worldwide support is provided by experienced application scientists and technical service personnel. Agilent's leading-edge R&D laboratories ensure the continued, timely introduction and optimization of innovative, easy-to-use nanomeasure system technologies.

[www.agilent.com/find/nano](http://www.agilent.com/find/nano)

### Americas

|               |                |
|---------------|----------------|
| Canada        | (877) 894 4414 |
| Latin America | 305 269 7500   |
| United States | (800) 829 4444 |

### Asia Pacific

|           |                |
|-----------|----------------|
| Australia | 1 800 629 485  |
| China     | 800 810 0189   |
| Hong Kong | 800 938 693    |
| India     | 1 800 112 929  |
| Japan     | 0120 (421) 345 |
| Korea     | 080 769 0800   |
| Malaysia  | 1 800 888 848  |
| Singapore | 1 800 375 8100 |
| Taiwan    | 0800 047 866   |
| Thailand  | 1 800 226 008  |

### Europe & Middle East

|                |                       |
|----------------|-----------------------|
| Austria        | 43 (0) 1 360 277 1571 |
| Belgium        | 32 (0) 2 404 93 40    |
| Denmark        | 45 70 13 15 15        |
| Finland        | 358 (0) 10 855 2100   |
| France         | 0825 010 700*         |
|                | *0.125 €/minute       |
| Germany        | 49 (0) 7031 464 6333  |
| Ireland        | 1890 924 204          |
| Israel         | 972-3-9288-504/544    |
| Italy          | 39 02 92 60 8484      |
| Netherlands    | 31 (0) 20 547 2111    |
| Spain          | 34 (91) 631 3300      |
| Sweden         | 0200-88 22 55         |
| Switzerland    | 0800 80 53 53         |
| United Kingdom | 44 (0) 118 9276201    |

Other European Countries:

[www.agilent.com/find/contactus](http://www.agilent.com/find/contactus)

Product specifications and descriptions in this document subject to change without notice.

© Agilent Technologies, Inc. 2012

Printed in USA, July 13, 2012

5991-0866EN



Agilent Technologies